CHEMISTRY
A EUROPEAN JOURNAL

DOI: 10.1002/chem.200901481

Syntheses, Optical Properties, and Theoretical Investigation of Silafluorenes and Spirobisilafluorenes Bearing Electron-Donating Aminostyryl Arms around a Silafluorene Core

Tomohiro Agou,[a, b] Md. Delwar Hossain,[a, c] and Takayuki Kawashima*[a]

Abstract: π-Extended silafluorenes and spirobisilafluorenes bearing electron-donating aminostyryl substituents at the 2,7- or 3,6-positions were synthesized by a Horner–Wadsworth–Emmons reaction. The electronic influence of spirocyclic structure and substitution mode of the aminostyryl substituents was investigated by UV/Vis spectroscopy, which indicated the existence of a spiroconjugation effect in the 3,6-substituted spirobisilafluorene. They exhibited moderate to strong fluorescence emission, and the fluorescence properties were compatible with the UV/Vis absorption characteristics, except for the 3,6-substituted spirobisilafluorene, which showed relatively large enhancement of fluorescence quantum yield and Stokes shift. The influence of the spirocyclic structure and substitution mode on the photophysical properties of the silicon compounds was investigated by DFT calculations.

Keywords: conjugation · density functional calculations · fluorescence · silicon · spiro compounds

Introduction

π-Conjugated molecules containing main group elements (hetero-π-conjugated molecules) are expected to be powerful building blocks for optoelectronic materials.[1–3] Electronic interaction between main group elements and π orbitals on hydrocarbon frameworks raises the HOMO energy level or lowers the LUMO energy level and decreases HOMO–LUMO energy gaps.[4] The small HOMO–LUMO energy gaps provide hetero-π-conjugated molecules with useful optoelectronic properties, such as strong light absorption in the longer wavelength region, intense photoluminescence emission, and electron or hole transport.

Silicon has a special position as a component of organic functional materials, because incorporation of silicon atoms into π-conjugated systems can decrease LUMO energy levels substantially thanks to a strong σ*(Si–C)–π* hyperconjugation effect.[5] Its high abundance in the earth's crust is also advantageous from the point of view of applications.[6] Especially, silole[1b,5,7] and its benzo-fused derivatives (benzosilole[8] and dibenzosilole (silafluorene)[9]), are the most important silicon-containing π-conjugated systems, because of their improved optoelectronic properties. The Si–C bonds of the silole derivatives are fixed perpendicular to π orbitals on the ring, and thus σ*(Si–C)–π* hyperconjugation is effective. In addition, silafluorenes have further advantages over the other silole derivatives, including the rigidity and planarity of the silafluorene rings, synthetic versatility, and chemical stability, which have stimulated a number of studies on applying silafluorene to functional materials. The various silafluorene derivatives that have been synthesized include ladder-type silafluorenes[9e,10] and polymeric silafluorenes,[9a,d] and their optical and electronic properties have been revealed. However, spirobisilafluorene, a three-dimensionally expanded silafluorene derivative, has not attracted much attention as a component of organic optoelectronic materials until recently,[11] despite its interesting structural and electronic characteristics.

[a] Dr. T. Agou, Dr. M. D. Hossain, Prof. Dr. T. Kawashima
Department of Chemistry
Graduate School of Science
The University of Tokyo
7-3-1 Hongo, Bunkyo-ku, Tokyo 113-0033 (Japan)
Fax: (+81) 3-5800-6899
E-mail: takayuki@chem.s.u-tokyo.ac.jp

[b] Dr. T. Agou
Present address: Kyoto University Pioneering Research Unit for Next Generation
Institute for Chemical Research, Kyoto University
Gokasho, Uji, Kyoto 611-0011 (Japan)

[c] Dr. M. D. Hossain
Present address: Department of Chemistry and Applied Chemistry
Graduate School of Science and Engineering, Saga University
1 Honjo-machi, Saga-city, Saga 840-8502 (Japan)

Supporting information for this article is available on the WWW under http://dx.doi.org/10.1002/chem.200901481.

Spirobisilafluorene can be recognized as a hybrid of silafluorene and spirobifluorene.[12] Spirobifluorene has a small HOMO–LUMO energy gap and good photoluminescence properties, owing to a spiroconjugation effect that raises its HOMO and delocalizes π electrons over the two biphenylene units. With regard to its solid-state properties, its rigid and pseudotetrahedral structure enhances amorphousness in the solid state, an important feature for organic thin-film devices. The combination of these properties with the σ(Si–C)*–π* hyperconjugation effect of silafluorene is expected to yield excellent materials with decreased HOMO–LUMO energy gaps, and spirobisilafluorene-based conjugated molecules are therefore candidates for organic optoelectronic materials. For this purpose, the effects of the spiro structure and the substitution pattern of the π-conjugated systems on the optoelectronic properties of spirobisilafluorene must be studied systematically, because this information is essential for molecular design of spirobisilafluorene derivatives with desired properties. However, the optical properties of silafluorenes and the corresponding spirobisilafluorenes have not been directly compared. In addition, almost all silafluorenes and spirobisilafluorenes have π-conjugated systems at their 2,7-positions, and thus the effect of the substitution pattern can not be elucidated.[13] Here we report an investigation of the influence of spirocyclic framework and substitution pattern on the photophysical properties of spirobisilafluorene derivatives, by using optical spectroscopy and theoretical calculations.

Our silafluorenes and spirobisilafluorenes designed for systematically studying the optical properties of spirobisilafluorenes are shown in Scheme 1. By comparison of the optical properties of silafluorenes **1** and **3** with those of spirobisilafluorenes **2** and **4**, respectively, the effect of the spirocyclic framework on their photophysical properties can be revealed. The electronic effect of the substitution pattern of the π systems can be clarified by comparisons between 3,6-substituted compounds **1** and **2** and 2,7-substituted compounds **3** and **4**. We selected electron-donating aminostyryl groups as π-conjugated substituents on the silafluorene rings, because donor–acceptor interactions between them and the silafluorene cores should provide improved UV/Vis absorption and fluorescence properties.

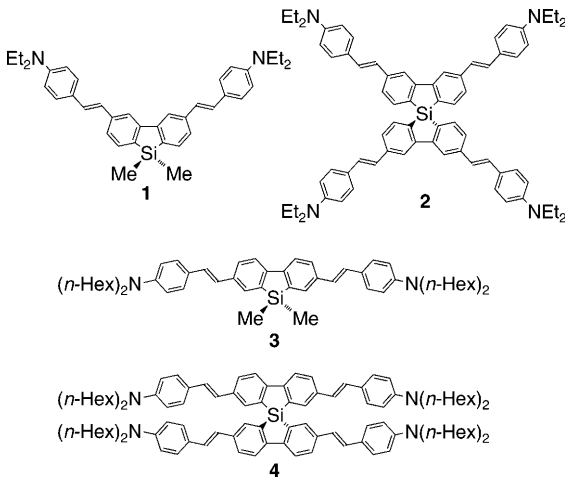

Scheme 1. 3,6-Substituted silafluorene **1**, 3,6-substituted spirobisilafluorene **2**, 2,7-substituted silafluorene **3**, and 2,7-substituted spirobisilafluorene **4**.

Results and Discussion

Syntheses: 3,6-Substituted silafluorene **1** and spirobisilafluorene **2** were synthesized by using the Horner–Wadsworth–Emmons (HWE) reaction as a key step (Scheme 2).

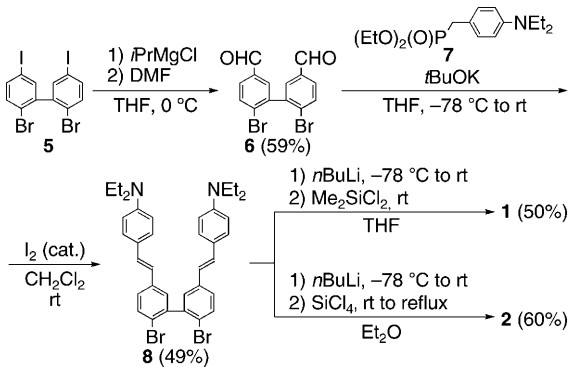

Scheme 2. Synthesis of 3,6-substituted silafluorene **1** and spirobisilafluorene **2**.

Starting from 2,2′-dibromo-5,5′-diiodobiphenyl (**5**), iodine–magnesium exchange reaction followed by treatment with DMF gave 2,2′-dibromo-5,5′-diformylbiphenyl (**6**).[14] The HWE reaction of **6** with phosphonate **7** in THF afforded **8**, a precursor of the 3,6-substituted compounds, as a *cis*/*trans* mixture (>95% *trans*, determined by ^{1}H NMR spectroscopy), and iodine-catalyzed isomerization of the crude material in CH_2Cl_2 provided pure **8** (all-*trans* form) in 49% yield. Treatment of **8** with *n*BuLi and Me_2SiCl_2 in THF produced silafluorene **1** in 50% yield as a light yellow-green solid after column chromatography on silica gel. Spirobisilafluorene **2** was obtained from **8** under the same conditions. After addition of $SiCl_4$ to a yellow solution of the dilithio derivative of **8**, the mixture was heated to reflux to give **2** as a yellow solid (60%). Compounds **1** and **2** are highly soluble in common organic solvents, and **2** even dissolves in hexane. Its spirocyclic structure may inhibit intermolecular interactions in the solid state and enhance amorphousness and solubility.

2,7-Substituted silafluorene **3** and spirobisilafluorene **4** were synthesized by a similar procedure (Scheme 3). Treatment of **12** with *n*BuLi followed by reaction with Me_2SiCl_2 and $SiCl_4$ gave silafluorene **3** and spirobisilafluorene **4**, respectively. Both silicon compounds were obtained as deep yellow solids, and their solubility was lower than those of **1** and **2**, in spite of the longer alkyl chains on the nitrogen atoms.

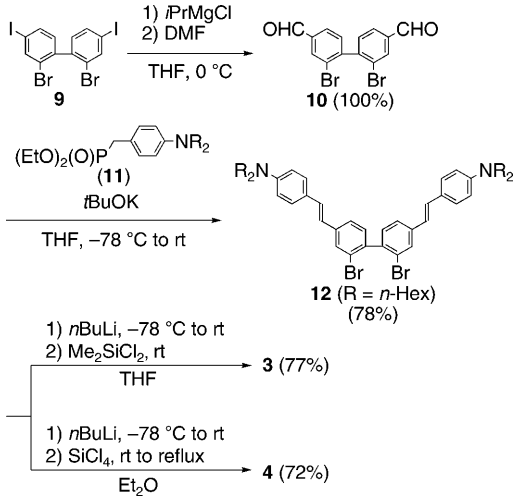

Scheme 3. Synthesis of 2,7-substituted silafluorene **3** and spirobisilafluorene **4**.

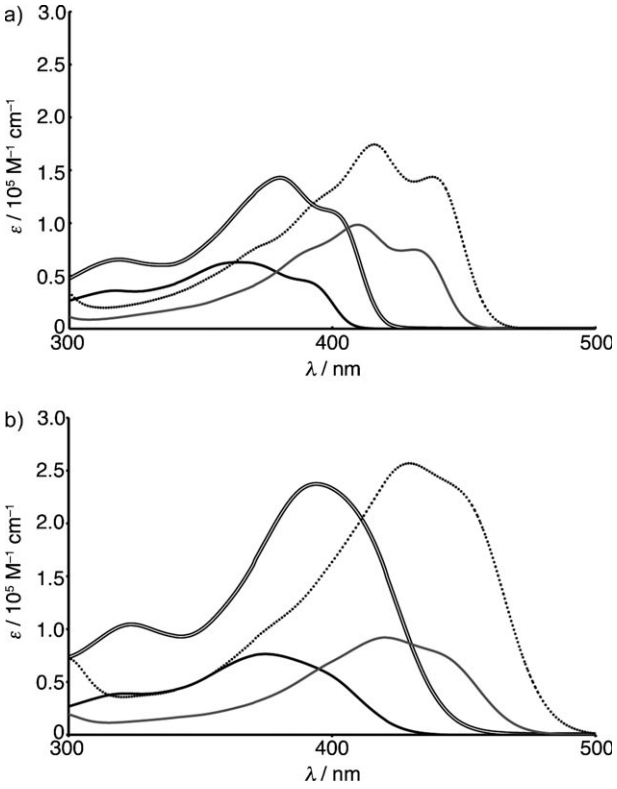

Figure 1. UV/Vis absorption spectra of **1**–**4** (black line: **1**, double line: **2**, gray line: **3**, dashed line: **4**). a) In cyclohexane. b) In CH_2Cl_2.

UV/Vis absorption characteristics: UV/Vis absorption spectra of silicon compounds **1**–**4** were measured in cyclohexane or CH_2Cl_2. The spectra are shown in Figure 1, and the optical data are summarized in Table 1.

In cyclohexane (Figure 1a), spirobisilafluorenes **2** and **4** exhibit a small bathochromic shift of the longest wavelength absorption peaks compared to those of silafluorenes **1** and **3**, respectively, that is, the spirobisilafluorenes have smaller HOMO–LUMO energy gaps. This may be ascribed to two effects: 1) The different types of substituents on the silicon atoms of the silafluorenes (one biarylene ligand and two methyl groups) and the spirobisilafluorenes (two biarylene ligands) influences the σ(Si–C)*–π* hyperconjugation effect and thus changes the LUMO energy levels. 2) Spiroconjugation between the two biarylene ligands of the spirobisilafluorenes elevates the HOMO energy levels. Both effects would contribute to smaller HOMO–LUMO energy gaps of spirobisilafluorene **2** or **4** compared with **1** or **3**, respectively. Therefore, σ(Si–C)*–π* hyperconjugation and spiroconjugation effects are thought to work synergistically and reduce the HOMO–LUMO energy gap, as anticipated in the Introduction, and this was further investigated theoretically (vide infra).

Table 1. Optical data of **1**–**4**.

	In cyclohexane					In CH_2Cl_2				
	λ_{max} [nm]	ε [10^5 M^{-1} cm^{-1}]	λ_{em} [nm]	Φ[a]	Stokes shift[b] [10^3 cm^{-1}]	λ_{max} [nm]	ε [10^5 M^{-1} cm^{-1}]	λ_{em} [nm]	Φ[a]	Stokes shift[b] [10^3 cm^{-1}]
1	365	0.63	406, 428	0.16	2.8	376	0.76	464	0.16	5.0
2	380	1.43	441	0.21	3.6	395	2.37	492	0.28	6.1
3	410	0.98	450, 476	0.74	2.2	421	0.92	503	0.76	3.8
4	416	1.74	458, 485	0.74	2.2	431	2.56	523	0.76	4.0

[a] Absolute quantum yields were recorded on a Hamamatsu Photonics Absolute Quantum Yield Determination System C9920-02. [b] Stokes shift $= 1/\lambda_{max} - 1/\lambda_{em}$.

Changing the solvent from cyclohexane to CH_2Cl_2 had little effect on the absorption wavelengths (Figure 1b, Table 1). Such small solvatochromic shifts indicate that the absorptions can be attributed to normal π–π*-type excitations rather than intramolecular charge transfer from the peripheral nitrogen atoms to the silafluorene cores.

As for the influence of the substitution pattern, compared with the 3,6-substituted compounds (**1** and **2**), the absorption maxima of the 2,7-substituted compounds (**3** and **4**) exhibited large bathochromic shifts indicating decreased HOMO–LUMO energy gaps of the latter compounds. In the case of the 2,7-substituted compounds, the π orbitals on the biarylene ligands are more efficiently delocalized over the aminostyryl substituents and the central biphenyl moieties, because the 4,4′-biphenylene linkage in **3** and **4** is a better π connecting unit than the 3,3′-biphenylene linkage in **1** and **2**.

Fluorescence properties: Fluorescence spectra of **1**–**4** were recorded in cyclohexane or CH_2Cl_2 (Figure 2), and the data are included in Table 1.

In cyclohexane, the fluorescence quantum yields of 3,6-substituted compounds **1** and **2** are smaller than those of 2,7-substituted compounds **3** and **4**. The larger Stokes shifts

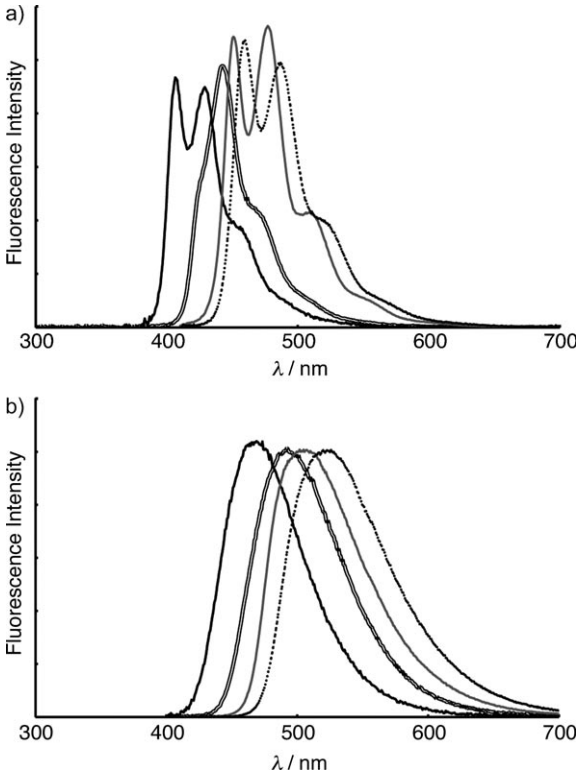

Figure 2. Fluorescence spectra of **1**–**4** (black line: **1**, double line: **2**, gray line: **3**, dashed line: **4**). a) In cyclohexane. b) In CH_2Cl_2.

in **1** and **2** mean that the structural change from the Frank–Condon states to the emissive states is considerable in **1** and **2**. Because their aminostyryl substituents are not strongly fixed in planarity due to the weak π conjugation through the 3,3′-biarylene linkage, conformational change in the excited states can easily occur. The many degrees of freedom of internal rotations and vibrations also dissipate the excitation energy via nonradiative paths, and this results in low fluorescence quantum yields.

On the other hand, the improved fluorescence quantum yields in **3** and **4** may be the result of expansion of π conjugation over the biarylene ligands, confirmed by UV/Vis spectroscopy. In general, broadening of π-conjugated systems is related to an increase in the transition dipole moment between the ground state and the excited states, which results in enhancement of fluorescence quantum yield.[15] Extension of the π systems also improves the molecular planarity in both ground and excited states and prohibits structural relaxation to some extent, and thus a decrease in the Stokes shifts results.

In the case of the 2,7-substituted compounds, the effect of the spirocyclic structure on the fluorescence emission is very small, since the fluorescence properties of **3** and **4** are very similar, except for the small redshift of the emission maxima of **4**. On the other hand, 3,6-substituted spirobisilafluorene **2** exhibited a slight improvement in fluorescence quantum yield and larger Stokes shift compared to corresponding silafluorene **1** in addition to the change in fluorescence band shape.

In CH_2Cl_2, the fluorescence spectra of **1**–**4** completely lost their vibrational structure, and the emission maxima were redshifted compared to fluorescence in cyclohexane. This indicates a more polar nature of the emissive states compared to the Frank–Condon states. The emission maxima of 3,6-substituted compounds **1** and **2** showed larger solvatochromic shifts than those of **3** and **4**, and thus **1** and **2** have much more polarized emissive states. The fluorescence quantum yields of compounds **1**–**4** in CH_2Cl_2, however, were almost the same as those in cyclohexane.

Theoretical calculations: To gain further insight into the optoelectronic properties of the silicon compounds, DFT calculations were performed at the B3LYP/6-31G(d) level of theory.[16] All calculations were carried out with the Gaussian 03 program package,[17] and Kohn–Sham orbitals were visualized with GaussView 4.1.[18] To reduce the computational burden, model compounds **1′**–**4′** (Scheme 4), which

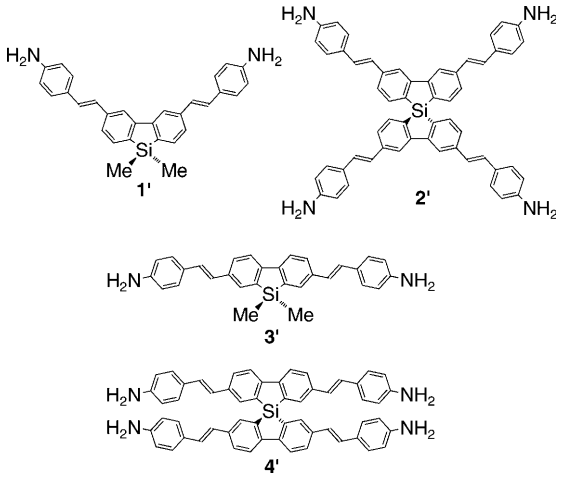

Scheme 4. Model compounds **1′**–**4′** employed in theoretical calculations.

have NH_2 groups instead of the NR_2 groups in the real molecules, were employed, and molecular symmetry was imposed in all calculations (**1′**: C_2, **2′**: D_2, **3′**: C_2, **4′**: S_4).

Energy diagrams of frontier orbitals are shown in Figure 3. For silafluorenes **1′** and **3′**, only HOMO and LUMO orbital energy levels are shown. For spirobisilafluorenes **2′** and **4′**, HOMO−1 and LUMO+1 energy levels are also shown in addition to those of the HOMO and LUMO. In the case of **2′**, LUMO and LUMO+1 are degenerate, but the energy gap between HOMO and HOMO−1 is small ($\Delta E = 0.11$ eV). On the contrary, not only LUMOs but also the HOMOs of **4′** are degenerate. The origin of this difference is discussed below.

Corresponding to the bathochromic shift of the absorption maximum, the HOMO–LUMO energy gap of spirobisilafluorene **2′** is smaller than that of silafluorene **1′**, due to the rise of the HOMO and fall of the LUMO. The fall in

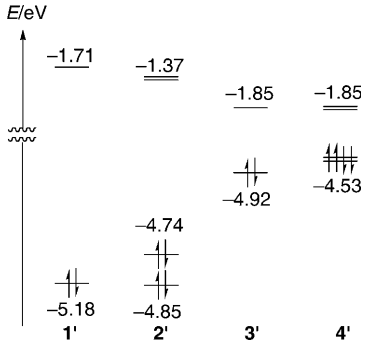

Figure 3. Energy diagram of frontier orbitals of **1′**-**4′**.

the LUMO may be due to the different substituents on the silicon atoms of **1′** and **2′**, which affect the extent of σ(Si–C)*–π* hyperconjugation. The rise of the HOMO of **2′** may originate from spiroconjugation between the highest occupied π orbitals on the two biarylene ligands, as revealed by the plots of the HOMO and HOMO−1 of **2′** (Figure 4). In

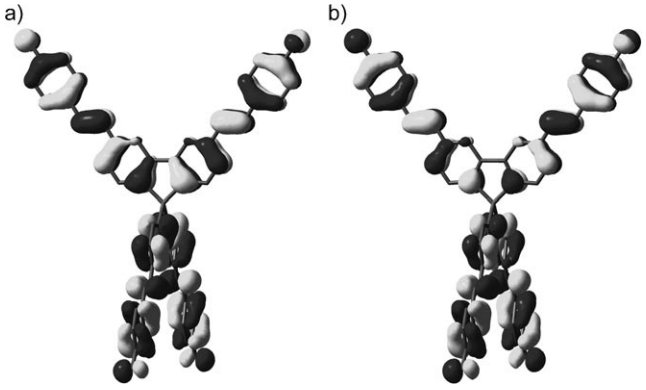

Figure 4. Kohn–Sham orbitals of **2′**. a) HOMO. b) HOMO−1. Hydrogen atoms are not shown.

the HOMO, two π orbitals on the two biarylene ligands interact with each other in an antibonding fashion, that is, the phases of the two π orbitals are not matched. On the other hand, the two π orbitals interact with each other in a bonding fashion in the HOMO−1, judging from the phases of the two orbitals. These findings mean that the π orbitals on the two biarylene ligands are mixed to form two delocalized π orbitals, HOMO and HOMO−1. Although the splitting between HOMO and HOMO−1 is not so large ($\Delta E = 0.11$ eV) as that of spirobifluorene ($\Delta E = 0.27$ eV, calculated at the B3LYP/6-31G(d) level of theory), such orbital interaction clearly indicates the existence of spiroconjugation in **2′**, which results in an increase in the HOMO energy level compared with **1′**. The weak spiroconjugation in **2′** should originate from long bonds between silicon and carbon atoms, because the overlap of the two π orbitals is affected by the distance between them.

Compared with 3,6-substituted compounds **1′** and **2′**, 2,7-substituted counterparts **3′** and **4′** have higher HOMOs and lower LUMOs, compatible with the observed bathochromic shifts in the UV/Vis spectra. This is due to the difference in π-orbital delocalization between the 3,6- and 2,7-substituted biarylene ligands. The latter system enhances π conjugation, since the 4,4′-biarylene linkage is a better π spacer than the 3,3′-biarlylene spacer. On the other hand, considering the difference in electronic structure of **3′** and **4′**, **4′** hardly benefits from its spirocyclic structure, unlike **2′**. The HOMO and HOMO−1 of **4′** are degenerate, unlike those of **2′**, that is, spiroconjugation is not effective in the 2,7-substituted spirobisilafluorene. Because the optimized geometries around the central silicon atoms of **2′** and **4′** are almost the same, geometrical reasons, such as the distance between the two biarylene ligands, can not explain the weak spiroconjugation in **4′**. Therefore, the difference in the electronic structure should be the main reason. The HOMO of **1′** (a model for half of **2′**) is fairly distributed over carbon atoms C8a and C9a. Accordingly, in **2′**, the spiroconjugation is effective due to efficient orbital overlap of the two π orbitals on the biarylene ligands. In contrast, the HOMO of **3′** (a model for half of **4′**) has smaller lobes on C8a and C9a, which result in decreased spiroconjugation efficiency in **4′**.

The results of the TDDFT calculations are summarized in Table 2. The calculated absorption wavelengths agreed moderately well with the experimental ones (Table 1). Because

Table 2. Results of the TDDFT calculations.[a]

	λ [nm]	f[b]	Excited state
1′	388	0.4595	LUMO←HOMO
	372	0.1877	LUMO←HOMO−1, LUMO+1←HOMO
2′	408	0.2361	LUMO←HOMO
	408	0.2385	LUMO+1←HOMO
	391	0.2369	LUMO←HOMO−1
	391	0.2342	LUMO+1←HOMO−1
	387	1.1453	LUMO+1←HOMO−2, LUMO←HOMO−3
3′	437	2.0684	LUMO←HOMO
4′	453	0.0892	LUMO←HOMO−1, LUMO+1←HOMO−1,
	(2 excitations)		LUMO←HOMO, LUMO+1←HOMO
	443	1.7616	LUMO←HOMO−1, LUMO+1←HOMO−1,
	(2 excitations)		LUMO←HOMO, LUMO+1←HOMO

[a] The TDDFT calculations were performed at the B3LYP/6-31G(d) level of theory. Only singlet excited states were calculated. [b] Oscillator strength.

4′ has degenerate HOMOs and LUMOs, the TDDFT calculation predicted two sets of degenerate excitations. All calculated excitation energies were smaller than the experimental values by about 10^3 cm^{-1}, probably because the calculations were performed on the optimized geometries with completely planar π systems, and hence π conjugation was overestimated. The calculations reproduced the redshifts of the longest absorption maxima of 2,7-substituted compounds **3** and **4** compared to 3,6-subsituted compounds **1** and **2**.

More importantly, the calculations confirmed that spirobisilafluorenes **2′** and **4′** have longer absorption wavelengths (**2′**: 408 nm, **4′**: 453 nm) than silafluorenes **1′** and **3′** (**1′**: 388 nm, **3′**: 437 nm), respectively, which reveals the influence of the spirocyclic structure on the UV/Vis absorption properties. The strongest optical transitions of 2,7-substituted compounds **3′** (437 nm) and **4′** (443 nm) have higher oscillator strengths than those of 3,6-substituted compounds **1′** (388 nm) and **2′** (408 nm), in accordance with the higher fluorescence quantum yields of the former pair. Especially, **4′** has several allowed optical transitions around 450 nm, and this may be the reason for its highly intense light absorption.

In summary, 2,7-substituted compounds **3′** and **4′** have smaller HOMO–LUMO energy gaps and redshifted absorption maxima compared to 3,6-substituted compounds **1′** and **2′**, which is comprehensible by considering the difference in π-conjugation efficiency between the 4,4′-biarylene units of **3′** and **4′** and the 3,3′-biarylene units of **1′** and **2′**. However, the theoretical calculations also showed that spiroconjugation does not contribute to the electronic properties of **4′** very much, unlike **2′**, and the two biaryl units of **4′** may be described as independent of each other rather than electronically coupled. On the other hand, **2′** was shown to have spiroconjugation between the two biaryl units in addition to σ*(Si–C)–π* hyperconjugation, and thus this substitution pattern can be useful for three-dimensional delocalization of π electrons through these two conjugation effects.

Conclusions

We have synthesized silafluorenes and spirobisilafluorenes bearing electron-donating aminostyryl groups at the periphery using the Horner–Wadsworth–Emmons reaction. Incorporation of the spirocyclic structure bathochromically shifted the UV/Vis absorption maxima because of the synergetic effect of σ(Si–C)*–π* hyperconjugation and spiroconjugation, confirmed by theoretical calculations. The substitution mode of the aminostyryl groups also affects optical properties, reflecting the efficiency of π conjugation. The silicon compounds exhibit moderate to strong fluorescence in the blue to green region, and the fluorescence properties were also affected by both the spirocyclic structure and the substitution pattern of the aminostyryl groups. Theoretical calculations on the silicon compounds revealed the influence of spiroconjugation around the central silicon atoms on their electronic states and photoexcitation behavior.

Experimental Section

General remarks: Commercial chemicals were used as received. Spectrochemical-grade dichloromethane (Dojindo) was used for optical measurements. All manipulations were performed under argon atmosphere using standard Schlenck techniques. Dehydrated solvents (THF and Et_2O) were purchased from Kanto Chemicals and further purified with an MBRAUN MB-SPS system equipped with activated alumina and molecular sieve columns before use, and other solvents were purified by common methods. Column chromatography was carried out with Kanto Silica Gel 60N. Gel permeation liquid chromatography (GPLC) was performed on Japan Analytical Industry LC-918 and LC-908 with JAIGEL 1H+2H columns and chloroform as a solvent. ^{1}H and ^{13}C NMR spectra were recorded on a Bruker DRX-500 spectrometer, and ^{29}Si NMR spectra were recorded on a JEOL AL-400 spectrometer. Tetramethylsilane was used as external standard for ^{1}H, ^{13}C, and ^{29}Si NMR spectroscopy. Low-resolution mass spectra were measured with a JEOL JMS-700P mass spectrometer (FAB positive) with *m*-nitrobenzyl alcohol or 2-nitrophenyl octyl ether as matrix. High-resolution mass spectra were recorded on a JEOL JMS-700P mass spectrometer (FAB positive) by using *m*-nitrobenzyl alcohol or 2-nitrophenyl octyl ether as matrix and PEG-600 or Ultramark as external standard. UV/Vis spectra were recorded on a JASCO V-670 spectrophotometer, and fluorescence spectra were measured with a JASCO FP-6500 fluorescence spectrophotometer. Fluorescence quantum yield was determined by a conventional comparison method with a JASCO FP-6500 fluorescence spectrophotometer or an absolute method with a Hamamatsu Photonics Absolute Quantum Yield Measurement System C9920-02 equipped with an integral sphere. All melting points were determined on a Yanaco MP-S3 micro melting point apparatus and are uncorrected. Elemental analyses were performed by the Microanalytical Laboratory of Department of Chemistry, Faculty of Science, the University of Tokyo. 2,2′-Dibromo-5,5′-diiodobiphenyl (**5**),[13] diethyl 4-(diethylamino)benzylphosphonate (**7**),[19] diethyl 4-(di-*n*-hexylamino)benzylphosphonate (**11**),[20] and 2,2′-dibromo-4,4′-diiodobiphenyl (**9**)[21] were prepared according to literature procedures.

2,2′-Dibromo-5,5′-diformylbiphenyl (6): At 0 °C, *i*PrMgCl (2.0 M in THF, 32 mL, 64 mmol) was added to a solution of **5** (15 g, 26 mmol) in THF (400 mL). After the mixture had been stirred for 20 min, DMF (5.0 mL, 65 mmol) was added slowly to the solution, and the mixture was allowed to warm to room temperature. After stirring for 12 h, the reaction was quenched with aqueous NH_4Cl. The mixture was extracted with dichloromethane, and the organic layer was dried over anhydrous $MgSO_4$. After filtration, the solvents were removed under reduced pressure. The crude product was recrystallized from ethanol to give **7** as a colorless solid (5.7 g, 59 %). M.p. 151–152 °C; ^{1}H NMR (500 MHz, $CDCl_3$, 25 °C, TMS): δ = 10.04 (s, 2H), 7.88 (d, J = 8.2 Hz, 2H), 7.80 (dd, J = 8.2, 2.0 Hz, 2H), 7.75 ppm (d, J = 2.0 Hz, 2H); ^{13}C NMR (126 MHz, $CDCl_3$, 25 °C, TMS): δ = 190.7, 141.8, 135.4, 133.8, 131.7, 130.5, 130.3 ppm; elemental analysis calcd (%) for $C_{14}H_8Br_2O_2$: C 45.69, H 2.19; found: C 45.46, H 2.29.

2,2′-Dibromo-5,5′-bis[4-(diethylamino)styryl]biphenyl (8): At −78 °C, *t*BuOK (5.4 g, 48 mmol) was slowly added to a mixture of **6** (3.4 g, 9.3 mmol), **7** (5.6 g, 19 mmol), and THF (300 mL), and the mixture was stirred for 12 h at room temperature. The solvent was removed under reduced pressure, and water was added to the residue. The mixture was extracted with dichloromethane, and the organic layer was dried over anhydrous $MgSO_4$ and filtered. After removal of the solvent under reduced pressure, the crude mixture was subjected to column chromatography (dichloromethane/hexane = 1/1) to give a light greenish solid containing a trace amount of *cis* isomers (confirmed by ^{1}H NMR spectroscopy). This mixture was stirred with iodine (0.35 g, 1.4 mmol) in toluene (20 mL) and dichloromethane (20 mL) at room temperature for 24 h. The reaction was quenched with aqueous Na_2SO_3. The aqueous layer was extracted with dichloromethane, and the combined organic layer was dried over anhydrous $MgSO_4$ and filtered. The solvents were removed under reduced pressure to give **8** as a yellow solid (3.0 g, 49 %). M.p. 184–185 °C; ^{1}H NMR (500 MHz, $CDCl_3$, 25 °C, TMS): δ = 7.60 (d, J = 8.3 Hz, 2H), 7.35 (m, 8H), 7.05 (d, J = 16.2 Hz, 2H), 6.84 (d, J = 16.2 Hz, 2H), 6.65 (d, J = 8.7 Hz, 4H), 3.40 (q, J = 6.9 Hz, 8H), 1.20 ppm (t, J = 6.9 Hz, 12H); ^{13}C NMR (126 MHz, $CDCl_3$, 25 °C, TMS): δ = 147.6, 142.2, 137.6, 132.6, 130.0, 128.2, 128.0, 126.6, 124.2, 122.0, 120.9, 111.6, 44.4, 12.6 ppm; elemental analysis calcd (%) for $C_{36}H_{38}Br_2N_2$: C 65.66, H 5.82, N 4.25; found: C 65.39, H 5.85, N, 3.99.

2,2′-Dibromo-4,4′-diformylbiphenyl (10): At 0 °C, *i*PrMgCl (2.0 M in THF, 8.5 mL, 17 mmol) was added to a solution of **9** (4.6 g, 8.2 mmol) in THF (100 mL). After the mixture had been stirred for 1 h, DMF (1.5 mL, 20 mmol) was added slowly to the reaction mixture. The solution was

gradually warmed to room temperature, and after stirring for 1 h, the reaction was quenched with aqueous NH_4Cl. The mixture was extracted with dichloromethane, and the organic layer was dried over anhydrous $MgSO_4$ and filtered. The solvents were removed under reduced pressure to give **10** as a colorless solid (3.0 g, 100%), and the crude material was used for the next step directly. M.p. 171–173°C; ^{1}H NMR (500 MHz, $CDCl_3$, 25°C, TMS): δ = 10.03 (s, 2H), 8.19 (d, J=1.5 Hz, 2H), 7.91 (dd, J=7.8, 1.5 Hz, 2H), 7.40 ppm (d, J=7.8 Hz, 2H); ^{13}C NMR (126 MHz, $CDCl_3$, 25°C, TMS): δ=190.2, 146.6, 137.5, 133.8, 131.2, 128.3, 123.9 ppm; HRMS (FAB$^+$): m/z calcd for $C_{14}H_8{}^{79}Br^{81}BrO_2$: 367.8871, found: 367.8850.

2,2′-Dibromo-4,4′-bis[4-(di-*n*-hexylamino)styryl]biphenyl (12): At −78°C, *t*BuOK (2.7 g, 24 mmol) was slowly added to a mixture of **10** (3.0 g, 8.2 mmol), **11** (7.0 g, 17 mmol), and THF (100 mL), and the mixture was warmed to room temperature and stirred for 48 h. The solvent was removed under reduced pressure, and water added to the residue. The mixture was extracted with dichloromethane, and the organic layer dried over anhydrous $MgSO_4$ and filtered. After removal of the solvent under reduced pressure, the crude mixture was recrystallized from hexane to give **12** as a yellow-green solid (5.6 g, 78%). M.p. 71–72°C; ^{1}H NMR (500 MHz, $CDCl_3$, 25°C, TMS): δ=7.83 (d, J=1.4 Hz, 2H), 7.50 (d, J=8.0 Hz, 2H), 7.45 (d, J=8.8 Hz, 4H), 7.26 (dd, J=8.0, 1.4 Hz, 2H), 7.14 (d, J=16.7 Hz, 2H), 6.89 (d, J=16.7 Hz, 2H), 6.69 (d, J=8.8 Hz, 4H), 3.35 (t, J=7.4 Hz, 8H), 1.66 (br, 8H), 1.39 (br, 24H), 0.97 ppm (t, J=6.8 Hz, 12H); ^{13}C NMR (126 MHz, $CDCl_3$, 25°C, TMS): δ=148.0, 139.9, 139.6, 131.2, 130.6, 129.5, 128.0, 124.5, 123.9, 123.8, 121.4, 111.5, 51.1, 31.7, 27.3, 26.8, 22.7, 14.1 ppm; HRMS (FAB$^+$): m/z calcd for $C_{52}H_{70}{}^{79}Br^{81}BrN_2$ 882.3885, found: 882.3862.

3,6-Bis[4-(diethylamino)styryl]-9,9-dimethylsilafluorene (1): *n*BuLi (1.53 M in hexane, 0.34 mL, 0.52 mmol) was added at −78°C to a solution of **8** (0.17 g, 0.26 mmol) in THF (20 mL), and the resulting solution was stirred for 30 min at room temperature. A solution of Me_2SiCl_2 (33 mL, 0.27 mmol) in THF (10 mL) was added to the solution, and the mixture was stirred for 20 h. The reaction was quenched with water. The aqueous layer was extracted with dichloromethane, and the organic layer dried over anhydrous $MgSO_4$ and filtered. After removal of the solvents under reduced pressure, the residue was separated by column chromatography (hexane/EtOAc=10/1) to give **1** as a light yellow-green solid (85 mg, 50%). M.p. 101–102°C; ^{1}H NMR (500 MHz, $CDCl_3$, 25°C, TMS): δ= 8.00 (s, 2H), 7.59 (d, J=7.3 Hz, 2H), 7.47 (d, J=8.5 Hz, 4H), 7.42 (d, J=7.3 Hz, 2H), 7.23 (d, J=16.1 Hz, 2H), 7.04 (d, J=16.1 Hz, 2H), 6.73 (d, J=8.5 Hz, 4H), 3.44 (q, J=6.6 Hz, 8H), 1.23 (t, J=6.6 Hz, 12H), 0.46 ppm (s, 6H); ^{13}C NMR (126 MHz, $CDCl_3$, 25°C, TMS): δ=148.2, 147.4, 140.2, 137.5, 132.8, 129.3, 127.9, 125.1, 124.7, 124.0, 118.3, 111.7, 44.4, 12.6, −2.7 ppm; HRMS (FAB$^+$): m/z calcd for $C_{38}H_{44}N_2Si$: 556.3274, found: 556.3251; elemental analysis calcd (%) for $C_{38}H_{44}N_2Si$: C 81.96, H 7.96, N 5.03; found: C 81.76, H 7.97, N 4.84.

9,9′-Spirobi{3,6-bis[4-(diethylamino)styryl]silafluorene} (2): *n*BuLi (1.53 M in hexane, 0.68 mL, 1.0 mmol) was added to a suspension of **8** (0.34 g, 0.52 mmol) in Et_2O (20 mL) at −78°C, and the mixture was stirred for 6 h at room temperature. A solution of $SiCl_4$ (30 mL, 0.26 mmol) in Et_2O (10 mL) was added to the solution, and the reaction mixture was stirred for 1.5 h at room temperature and then heated to reflux for 12 h. The reaction was quenched with water. The aqueous layer was extracted with dichloromethane, and the organic layer was dried over anhydrous $MgSO_4$ and filtered. The solvents were removed under reduced pressure, and the crude material was separated by column chromatography (hexane/EtOAc=10/1) to give **2** as a light yellow solid (0.16 g, 60%). M.p. 192–193°C; ^{1}H NMR (500 MHz, $CDCl_3$, 25°C, TMS): δ=8.15 (s, 4H), 7.25–7.50 (m, 20H), 7.02 (d, J=16.3 Hz, 4H), 6.70 (d, J=8.6 Hz, 8H), 3.40 (q, J=6.6 Hz, 16H), 1.20 ppm (t, J=6.6 Hz, 24H); ^{13}C NMR (126 MHz, $CDCl_3$, 25°C, TMS): δ=150.3, 148.0, 141.3, 134.2, 131.4, 130.0, 128.0, 126.0, 124.1, 123.2, 118.1, 118.5, 44.3, 12.4 ppm; ^{29}Si NMR (99 MHz, $CDCl_3$, 25°C, TMS): δ=−8.34 ppm; HRMS (FAB$^+$) m/z calcd for $C_{72}H_{76}N_4Si$: 1024.5839, found: 1024.5870; elemental analysis calcd (%) for $C_{72}H_{76}SiN_4$: C 84.33, H 7.47, N 5.46; found: C 83.69, H 7.73, N, 5.33.

2,7-Bis{4-[di(*n*-hexyl)amino]styryl}-9,9-dimethylsilafluorene (3): At −78°C, *n*BuLi (1.57 M in hexane, 0.17 mL, 0.26 mmol) was added to a solution of **12** (0.12 g, 0.13 mmol) in THF (30 mL). The resulting mixture was stirred at this temperature for 30 min, and a solution of Me_2SiCl_2 (20 mL, 0.14 mmol) in THF (10 mL) was slowly added to the resulting mixture. The mixture was allowed to warm to room temperature and stirred for 20 h. The reaction was quenched with water. The aqueous layer was extracted with dichloromethane, and the organic layer was dried over anhydrous Mg_2SO_4 and filtered. The solvents were removed under reduced pressure, and the residue subjected to column chromatography (dichloromethane/hexane=3/7) to give **3** as yellow-green solid (80 mg, 77%). M.p. 112–113°C; ^{1}H NMR (500 MHz, $CDCl_3$, 25°C, TMS): δ=7.74 (d, J=7.5 Hz, 2H), 7.73 (s, 2H), 7.52 (d, J=7.5 Hz, 2H), 7.39 (d, J=8.6 Hz, 4H), 7.07 (d, J=16.2 Hz, 2H), 6.91 (d, J=16.2 Hz, 2H), 6.62 (d, J=8.6 Hz, 4H), 3.28 (t, J=7.5 Hz, 8H), 1.58 (br, 8H), 1.32 (br, 24H), 0.89 (t, J=6.9 Hz, 12H), 0.46 ppm (s, 6H); ^{13}C NMR (126 MHz, $CDCl_3$, 25°C, TMS): δ=147.7, 146.2, 139.3, 137.0, 130.1, 128.3, 128.0, 127.7, 124.6, 123.6, 120.9, 111.5, 51.0, 31.7, 27.3, 26.8, 22.7, 14.1, −3.1 ppm; HRMS (FAB$^+$) m/z calcd for $C_{54}H_{76}N_2Si$ 780.5778, found: 780.5761.

9,9′-Spirobi(2,7-bis{4-[di(*n*-hexyl)amino]styryl}silafluorene) (4): At −78°C, *n*BuLi (1.57 M in hexane, 0.5 mL, 0.79 mmol) was added dropwise to a solution of **12** (0.35 g, 0.39 mmol) in Et_2O (50 mL). The solution was allowed to warm to room temperature and stirred for 6 h. A solution of $SiCl_4$ (23 mL, 0.20 mmol) in Et_2O (10 mL) was added slowly to the resulting solution at room temperature. The reaction mixture was stirred at room temperature for 1.5 h and heated to reflux for 24 h. The reaction was quenched with water, and the aqueous layer was extracted with dichloromethane. The organic layer was dried over anhydrous $MgSO_4$ and filtered, and the organic solvents were removed under reduced pressure. The crude products were subjected to GPLC to give **4** as a yellow solid (0.21 g, 72%). M.p. 102–103°C; ^{1}H NMR (500 MHz, $CDCl_3$, 25°C, TMS): δ=7.88 (d, J=8.1 Hz, 4H), 7.61 (s, 4H), 7.58 (d, J=8.1 Hz, 4H), 7.28 (d, J=8.8 Hz, 8H), 6.97 (d, J=16.2 Hz, 4H), 6.79 (d, J=16.2 Hz, 4H), 6.55 (d, J=8.8 Hz, 8H) 3.23 (t, J=7.2 Hz, 16H), 1.54 (br, 16H), 1.29 (br, 48H), 0.87 ppm (t, J=6.4 Hz, 24H); ^{13}C NMR (126 MHz, $CDCl_3$, 25°C, TMS): δ=148.2, 147.6, 137.7, 133.3, 131.6, 129.3, 128.8, 127.7, 124.5, 123.0, 121.1, 111.4, 51.0, 31.7, 27.2, 26.8, 22.7, 14.0 ppm; HRMS (FAB$^+$) m/z calcd for $C_{104}H_{140}N_4Si$: 1474.0879, found: 1474.0802.

Acknowledgements

This work was partially supported by a Grants-in-Aid for the Global COE Program for Chemistry Innovation and Scientific Researches from MEXT and JSPS. We thank Tosoh Finechem Corp. and Shin-etsu Chemical Co. Ltd. for generous gifts of alkyllithiums and silicon reagents, respectively.

[1] a) S. Yamaguchi, K. Tamao, *Chem. Lett.* **2005**, *34*, 2; b) M. Hissler, P. W. Dyer, R. Réau, *Coord. Chem. Rev.* **2003**, *244*, 1.
[2] a) M. G. Hobbs, T. Baumgartner, *Eur. J. Inorg. Chem.* **2007**, 3611; b) T. Baumgartner, R Réau, *Chem. Rev.* **2006**, *106*, 4681; c) M. Hissler, P. W. Dyer, R. Réau, *Top. Curr. Chem.* **2005**, *250*, 127.
[3] a) A. Wakamiya, S. Yamaguchi, *J. Synth. Org. Chem. Jpn.* **2008**, *66*, 858; b) S. Yamaguchi, A. Wakamiya, *Pure Appl. Chem.* **2006**, *78*, 1413; c) C. D. Entwistle, T. B. Marder, *Chem. Mater.* **2004**, *16*, 4574.
[4] U. Salzner, J. B. Lagowski, P. G. Pickup, R. A. Poirier, *Synth. Met.* **1998**, *96*, 177.
[5] S. Yamaguchi, K. Tamao in *The Chemistry of Organic Silicon Compounds, Vol. 3* (Eds.: Z. Rappoport, Y. Apeloig), Wiley-Interscience, New York, **2001**, pp. 641–693.
[6] D. F. Shriver, P. W. Atkins, *Inorganic Chemistry*, 3rd ed., Oxford University Press, Oxford, **1999**.
[7] a) G. Yu, S.-W. Yin, Y.-Q. Liu, J.-S. Chen, X.-J. Xu, X.-B. Sun, D.-G. Ma, X.-W. Zhan, Q. Peng, Z.-G. Shuai, B.-Z. Tang, D.-B. Zhu, W.-H. Fang, Y. Luo, *J. Am. Chem. Soc.* **2005**, *127*, 6335; b) K. Tamao, S. Yamaguchi, *J. Organomet. Chem.* **2000**, *611*, 5.

[8] L. Ilies, H. Tsuji, Y. Sato, E. Nakamura, *J. Am. Chem. Soc.* **2008**, *130*, 4240.
[9] a) W. W. W. H. Wong, J. F. Hooper, A. B. Holmes, *Aust. J. Chem.* **2009**, *62*, 393; b) A. C. Grimsdale, K. L. Chan, R. E. Martin, P. G. Jokisz, A. B. Holmes, *Chem. Rev.* **2009**, *109*, 897; c) M. Shimizu, H. Tatsumi, K. Mochida, K. Oda, T. Hiyama, *Chem. Asian J.* **2008**, *3*, 1238; d) M. Shimizu, K. Mochida, T. Hiyama, *Angew. Chem.* **2008**, *120*, 9906; *Angew. Chem. Int. Ed.* **2008**, *47*, 9760; e) E. G. Wang, C. Li, W.-L. Zhuang, J.-B. Peng, Y. Cao, *J. Mater. Chem.* **2008**, *18*, 797; f) T. Matsuda, S. Kadowaki, T. Goya, M. Murakami, *Org. Lett.* **2007**, *9*, 133.
[10] L. Li, J. Xiang, C. Xu, *Org. Lett.* **2007**, *9*, 4877.
[11] S. H. Lee, B.-B. Jan, Z. H. Kafafi, *J. Am. Chem. Soc.* **2005**, *127*, 9071.
[12] T. P. I. Saragi, T. Spehr, A. Siebert, T. Fuhrmann-Lieker, J. Salbeck, *Chem. Rev.* **2007**, *107*, 1011.
[13] To our knowledge, there is only one report describing the synthesis and optical properties of 3,6-substituted silafluorenes: K. L. Chan, S. E. Watkins, C. S. K. Mak, M. J. McKiernan, C. R. Towns, S. I. Pascu, A. B. Holmes, *Chem. Commun.* **2005**, 5766. However, there has been no report on the corresponding spirobisilafluorenes.
[14] P. Knochel, D. Wolfgang, N. Gommermann, F. F. Kneisel, F. Kopp, T. Korn, I. Sapountzis, V. A. Vu, *Angew. Chem.* **2003**, *115*, 4438; *Angew. Chem. Int. Ed.* **2003**, *42*, 4302.
[15] B. Valeur, *Molecular Fluorescence*, Wiley-VCH, Weinheim, **2002**.
[16] a) R. E. Stratmann, G. E. Scuseria, M. J. Frisch, *J. Chem. Phys.* **1998**, *109*, 8218; b) R. Bauernschmitt, R. A. Ahlrichs, *Chem. Phys. Lett.* **1996**, *256*, 454; c) M. E. Casida, C. Jamorski, K. C. Casida, D. R. Salahub, *J. Chem. Phys.* **1998**, *108*, 4439.
[17] Gaussian 03, Revision D.02, M. J. Frisch, G. W. Trucks, H. B. Schlegel, G. E. Scuseria, M. A. Robb, J. R. Cheeseman, J. A. Montgomery, Jr., T. Vreven, K. N. Kudin, J. C. Burant, J. M. Millam, S. S. Iyengar, J. Tomasi, V. Barone, B. Mennucci, M. Cossi, G. Scalmani, N. Rega, G. A. Petersson, H. Nakatsuji, M. Hada, M. Ehara, K. Toyota, R. Fukuda, J. Hasegawa, M. Ishida, T. Nakajima, Y. Honda, O. Kitao, H. Nakai, M. Klene, X. Li, J. E. Knox, H. P. Hratchian, J. B. Cross, V. Bakken, C. Adamo, J. Jaramillo, R. Gomperts, R. E. Stratmann, O. Yazyev, A. J. Austin, R. Cammi, C. Pomelli, J. W. Ochterski, P. Y. Ayala, K. Morokuma, G. A. Voth, P. Salvador, J. J. Dannenberg, V. G. Zakrzewski, S. Dapprich, A. D. Daniels, M. C. Strain, O. Farkas, D. K. Malick, A. D. Rabuck, K. Raghavachari, J. B. Foresman, J. V. Ortiz, Q. Cui, A. G. Baboul, S. Clifford, J. Cioslowski, B. B. Stefanov, G. Liu, A. Liashenko, P. Piskorz, I. Komaromi, R. L. Martin, D. J. Fox, T. Keith, M. A. Al-Laham, C. Y. Peng, A. Nanayakkara, M. Challacombe, P. M. W. Gill, B. Johnson, W. Chen, M. W. Wong, C. Gonzalez, J. A. Pople, Gaussian, Inc., Wallingford CT, **2004**.
[18] GaussView, Version 4.1, R. Dennington II, T. Keith, J. Millam, Semichem, Inc., Shawnee Mission, **2007**.
[19] S. Zheng, S. Barlow, T. C. Parker, S. R. Marder, *Tetrahedron Lett.* **2003**, *44*, 7989.
[20] S. R. Hammond, O. Clot, K. Firestone, A. Kimberly, H. Denise, D. Lao, M. Haller, G. D. Gregory, B. Carlson, A. K.-Y. Alex, P. J. Reid, L. R. Dalton, *Chem. Mater.* **2008**, *20*, 3425.
[21] W. Huang, R.-F. Chen, Q. Fan, H.-J. Jiang, C. Zheng (Nanjing University of Posts and Telecommunications, China), CN 101298459, **2008**.

Received: June 2, 2009
Revised: September 10, 2009
Published online: November 13, 2009

